International Journal of Modern Physics B
Vol. 24, Nos. 25 & 26 (2010) 5229–5239

DOI: 10.1142/S0217979210057353

World Scientific
www.worldscientific.com

SPIN SINGLET AND TRIPLET SUPERCONDUCTIVITY INDUCED BY CORRELATED HOPPING INTERACTIONS

LUIS A. PEREZ

Instituto de Física, Universidad Nacional Autónoma de México,
Apartado Postal 20-364, 01000, D.F., México
lperez@fisica.unam.mx

J. SAMUEL MILLAN

Facultad de Ingeniería, Universidad Autónoma del Carmen,
Cd. del Carmen, 24180, Campeche, México
smillan@pampano.unacar.mx

CHUMIN WANG

Instituto de Investigaciones en Materiales, Universidad Nacional Autónoma de México,
Apartado Postal 70-360, 04510, D.F., México
chumin@servidor.unam.mx

Received 15 November 2009

In this article, we show that the Bardeen-Cooper-Schrieffer (BCS) formalism applied to a Hubbard model is capable to predict the *s*-, *p*- and *d*-wave superconductivity within a single theoretical scheme. This study is performed on a square lattice described by a generalized Hubbard Hamiltonian, in which correlated-hopping interactions are included in addition to the repulsive Coulombic one. Within the BCS formalism using a variable chemical potential, the superconducting ground states are determined by two coupled integral equations, whose integrand functions have main contributions around the Fermi surface. We observe the existence of a maximum critical temperature for *s*-, *p*- and *d*-wave superconducting channels that occur at the medium, low and high electron densities, respectively. Furthermore, the *p*- and *d*-wave superconducting specific heats show a power-law temperature dependence, instead of the exponential one for the *s* channel. Finally, the smallness of the anisotropic single-energy-excitation-gap minima is essential for the specific heat behavior, and this fact allows to understand the experimental data obtained from Sr_2RuO_4 and $La_{2-x}Sr_xCuO_4$ superconductors.

Keywords: Superconducting gap symmetry; Hubbard model; BCS theory.

1. Introduction

The theory developed by J. Bardeen, L. N. Cooper and J. R. Schrieffer (BCS) was very successful in explaining the main features of metallic superconductors.[1] In the last two decades, the observation of *d*-symmetry pairing in ceramic superconductors has motivated the research of models beyond the standard BCS theory to include

anisotropic superconducting gap symmetries.[2] The recent discovery of the p-wave spin-triplet superconducting state in Sr_2RuO_4 has highly enhanced this research.[3] The two-dimensional nature present in both p and d-wave superconducting systems could be essential for understanding their peculiarities. In general, the energy spectrum of elementary excitations in solids determines the temperature dependence of their specific heat, and for a superconductor it gives information regarding to the symmetry of its superconducting state. An s-wave superconductor has an exponentially temperature-dependent electronic specific heat, while an anisotropic nodal superconducting gap leads to a power-law dependence, as occur in the cuprate superconductors and in Sr_2RuO_4.[4] For these materials, three-band Hubbard models have been proposed to describe the dynamics of the carriers on the CuO_2 and RuO_2 planes,[5,6] and the electronic states close to the Fermi energy can be reasonably well described by a single-band tight-binding model on a square lattice with second neighbour hoppings.[5,7] In this article, we study s-, p- and d-wave superconducting states within a single-band generalized Hubbard Hamiltonian, in which nearest (Δt) and next-nearest (Δt_3) neighbour correlated-hopping interactions are considered in addition of the on-site (U) Coulombic interaction.[8] Certainly, Δt and Δt_3 are always present in real materials and in spite of having small strengths, they are essential in the determination of the superconducting symmetry.

2. The Model

We start from a single-band Hubbard model with on-site Coulombic interaction (U), first- (Δt) and second-neighbour (Δt_3) correlated-hopping interactions. The corresponding Hamiltonian can be written as

$$\hat{H} = t \sum_{\langle i,j\rangle,\sigma} c^{\dagger}_{i,\sigma} c_{j,\sigma} + t' \sum_{\langle\langle i,j\rangle\rangle,\sigma} c^{\dagger}_{i,\sigma} c_{j,\sigma} + U \sum_{i} n_{i,\uparrow} n_{i,\downarrow}$$
$$+\Delta t \sum_{\langle i,j\rangle,\sigma} c^{\dagger}_{i,\sigma} c_{j,\sigma} (n_{i,-\sigma} + n_{j,-\sigma}) + \Delta t_3 \sum_{\langle i,l\rangle,\langle j,l\rangle,\sigma,\langle\langle i,j\rangle\rangle} c^{\dagger}_{i,\sigma} c_{j,\sigma} n_l \quad , \qquad (1)$$

where $c^{\dagger}_{i,\sigma}$ ($c_{i,\sigma}$) is the creation (annihilation) operator with spin $\sigma = \downarrow$ *or* $\uparrow$ at site i, $n_{i,\sigma} = c^{\dagger}_{i,\sigma} c_{i,\sigma}$, $n_i = n_{i,\uparrow} + n_{i,\downarrow}$, $\langle i,j\rangle$ and $\langle\langle i,j\rangle\rangle$ denote respectively the nearest-neighbor and the next-nearest-neighbor sites. This model can lead to s- and d-wave superconducting ground states without attractive density-density interactions.[9] Let us start from a square lattice with lattice parameter a, where we further consider a small distortion of its right angles in order to include the possible existence of a bulk structural distortion in Sr_2RuO_4.[10] This distortion produces changes in the second-neighbour interactions, such as t' and Δt_3 terms in Eq. (1), and their new values are $t' \pm \delta$ and $\Delta t_3 \pm \delta_3$, where $\pm$ refers to the $\hat{x} \pm \hat{y}$ direction. Performing a Fourier transform, this Hamiltonian in the momentum space becomes

$$\hat{H} = \sum_{\mathbf{k},\sigma} \varepsilon_0(\mathbf{k}) c^{\dagger}_{\mathbf{k},\sigma} c_{\mathbf{k},\sigma}$$

$$+\frac{1}{N_s}\sum_{\mathbf{k},\mathbf{k}',\mathbf{q}} V_{\mathbf{k},\mathbf{k}',\mathbf{q}} c^{\dagger}_{\mathbf{k}+\mathbf{q},\uparrow} c^{\dagger}_{-\mathbf{k}'+\mathbf{q},\downarrow} c_{-\mathbf{k}'+\mathbf{q},\downarrow} c_{\mathbf{k}+\mathbf{q},\uparrow}$$

$$+\frac{1}{N_s}\sum_{\mathbf{k},\mathbf{k}',\mathbf{q},\sigma} W_{\mathbf{k},\mathbf{k}',\mathbf{q}} c^{\dagger}_{\mathbf{k}+\mathbf{q},\sigma} c^{\dagger}_{-\mathbf{k}'+\mathbf{q},\sigma} c_{-\mathbf{k}'+\mathbf{q},\sigma} c_{\mathbf{k}+\mathbf{q},\sigma} \quad , \tag{2}$$

where N_s is the total number of sites,

$$\varepsilon_0(\mathbf{k}) = 2t\left[\cos(k_x a) + \cos(k_y a)\right] + 2t'_+ \cos(k_x a + k_y a) + 2t'_- \cos(k_x a - k_y a)\,, \tag{3}$$

$$\begin{aligned} V_{\mathbf{k},\mathbf{k}'\mathbf{q}} = U &+ 2\Delta t\left[\beta(\mathbf{k}+\mathbf{q}) + \beta(-\mathbf{k}+\mathbf{q}) + \beta(\mathbf{k}'+\mathbf{q}) + \beta(-\mathbf{k}'+\mathbf{q})\right] \\ &+ \Delta t_3^{+}\left[\gamma(\mathbf{k}+\mathbf{q},\mathbf{k}'+\mathbf{q}) + \gamma(-\mathbf{k}+\mathbf{q},-\mathbf{k}'+\mathbf{q})\right] \\ &+ \Delta t_3^{-}\left[\zeta(\mathbf{k}+\mathbf{q},\mathbf{k}'+\mathbf{q}) + \zeta(-\mathbf{k}+\mathbf{q},-\mathbf{k}'+\mathbf{q})\right] \quad , \end{aligned} \tag{4}$$

and

$$W_{\mathbf{k},\mathbf{k}'\mathbf{q}} = \Delta t_3^{+}\gamma(\mathbf{k}+\mathbf{q},\mathbf{k}'+\mathbf{q}) + \Delta t_3^{-}\zeta(\mathbf{k}+\mathbf{q},\mathbf{k}'+\mathbf{q}) \quad , \tag{5}$$

being

$$\beta(\mathbf{k}) = 2\left[\cos(k_x a) + \cos(k_y a)\right] \quad , \tag{6}$$

$$\gamma(\mathbf{k},\mathbf{k}') = 2\cos(k_x a + k'_y a) + 2\cos(k'_x a + k_y a) \quad , \tag{7}$$

$$\zeta(\mathbf{k},\mathbf{k}') = 2\cos(k_x a - k'_y a) + 2\cos(k'_x a - k_y a) \quad . \tag{8}$$

and $2\mathbf{q}$ is the wave vector of the pair center of mass. After a standard Hartree-Fock decoupling of the interaction terms with $\mathbf{q} \neq 0$ applied to Eq. (2),[11] the reduced Hamiltonian for $\mathbf{q} = 0$ is

$$\hat{H} = \sum_{\mathbf{k},\sigma} \varepsilon(\mathbf{k}) c^{\dagger}_{\mathbf{k},\sigma} c_{\mathbf{k},\sigma} + \frac{1}{N_s}\sum_{\mathbf{k},\mathbf{k}'} V_{\mathbf{k},\mathbf{k}',\mathbf{0}} c^{\dagger}_{\mathbf{k},\uparrow} c^{\dagger}_{-\mathbf{k}',\downarrow} c_{-\mathbf{k}',\downarrow} c_{\mathbf{k},\uparrow}$$

$$+\frac{1}{N_s}\sum_{\mathbf{k},\mathbf{k}',\sigma} W_{\mathbf{k},\mathbf{k}',\mathbf{0}} c^{\dagger}_{\mathbf{k},\sigma} c^{\dagger}_{-\mathbf{k}',\sigma} c_{-\mathbf{k}',\sigma} c_{\mathbf{k},\sigma} \quad , \tag{9}$$

where the mean-field dispersion relation is given by

$$\begin{aligned} \varepsilon(\mathbf{k}) = n\frac{U}{2} &+ 2(t + n\Delta t)\left[\cos(k_x a) + \cos(k_y a)\right] + \\ &+ 2(t'_+ + 2n\Delta t_3^{+})\cos(k_x a + k_y a) + 2(t'_- + 2n\Delta t_3^{-})\cos(k_x a - k_y a) \quad . \end{aligned} \tag{10}$$

Notice that the single electron dispersion relation $\varepsilon(\mathbf{k})$ is now modified by adding terms $n\Delta t$, $2n\Delta t_3^{\pm}$ and $nU/2$ to the hoppings t, t' and the self-energy, respectively.

3. Coupled Integral Equations

Applying the BCS formalism to Eq. (9), we obtain the following two coupled integral equations,[8,9,12] which determine the anisotropic superconducting gap $[\Delta(\mathbf{k})]$ and the chemical potential (μ) for a given temperature (T) and electron density (n),

$$\Delta(\mathbf{k}) = -\frac{1}{2N_s}\sum_{\mathbf{k}'}\frac{Z_{\mathbf{k},\mathbf{k}'}\Delta(\mathbf{k}')}{E(\mathbf{k}')}\tanh\left(\frac{E(\mathbf{k}')}{2k_BT}\right) \quad , \tag{11}$$

and

$$n-1 = -\frac{1}{N_s}\sum_{\mathbf{k}}\frac{\varepsilon(\mathbf{k})-\mu}{E(\mathbf{k})}\tanh\left(\frac{E(\mathbf{k})}{2k_BT}\right) \quad , \tag{12}$$

where the single excitation energy is given by

$$E(\mathbf{k}) = \sqrt{(\varepsilon(\mathbf{k})-\mu)^2+\Delta^2(\mathbf{k})} \quad , \tag{13}$$

$Z_{\mathbf{k},\mathbf{k}'}$ and $\Delta(\mathbf{k})$ depend on the symmetry of superconducting ground states as given in Table 1.

Table 1. Interaction potentials $(Z_{\mathbf{k},\mathbf{k}'})$ and superconducting gaps $[\Delta(\mathbf{k})]$ as functions of pairing symmetry.

Symmetry	$Z_{\mathbf{k},\mathbf{k}'}$	$\Delta(\mathbf{k})$
s-wave	$V_{\mathbf{k},\mathbf{k}',\mathbf{0}}$	$\Delta_s + \Delta_s^*\,[\cos(k_xa)+\cos(k_ya)]$
p-wave	$W_{\mathbf{k},\mathbf{k}',\mathbf{0}}$	$\Delta_p\,[\sin(k_xa)\pm\sin(k_ya)]$
d-wave	$V_{\mathbf{k},\mathbf{k}',\mathbf{0}}$	$\Delta_d\,[\cos(k_xa)-\cos(k_ya)]$

For the s-wave case, Eq. (11) becomes *per se* two coupled equations[12]

$$\Delta_{s^*} = -4\Delta t_3\,(I_2\Delta_{s^*}+I_1\Delta_s) - 4\Delta t\,(I_1\Delta_{s^*}+I_0\Delta_s) \quad , \tag{14}$$

and

$$\Delta_s = -U\,(I_1\Delta_{s^*}+I_0\Delta_s) - 4\Delta t\,(I_2\Delta_{s^*}+I_1\Delta_s) \quad , \tag{15}$$

where

$$\begin{aligned} I_l &= \frac{1}{N_s}\sum_{\mathbf{k}}\frac{[\cos(k_xa)+\cos(k_ya)]^l}{2E(\mathbf{k})}\tanh\left(\frac{E(\mathbf{k})}{2k_BT}\right) \\ &= \frac{a^2}{8\pi^2}\int_{-\pi/a}^{\pi/a}\int_{-\pi/a}^{\pi/a}dk_xdk_y\frac{[\cos(k_xa)+\cos(k_ya)]^l}{E(\mathbf{k})}\tanh\left(\frac{E(\mathbf{k})}{2k_BT}\right) \quad , \end{aligned} \tag{16}$$

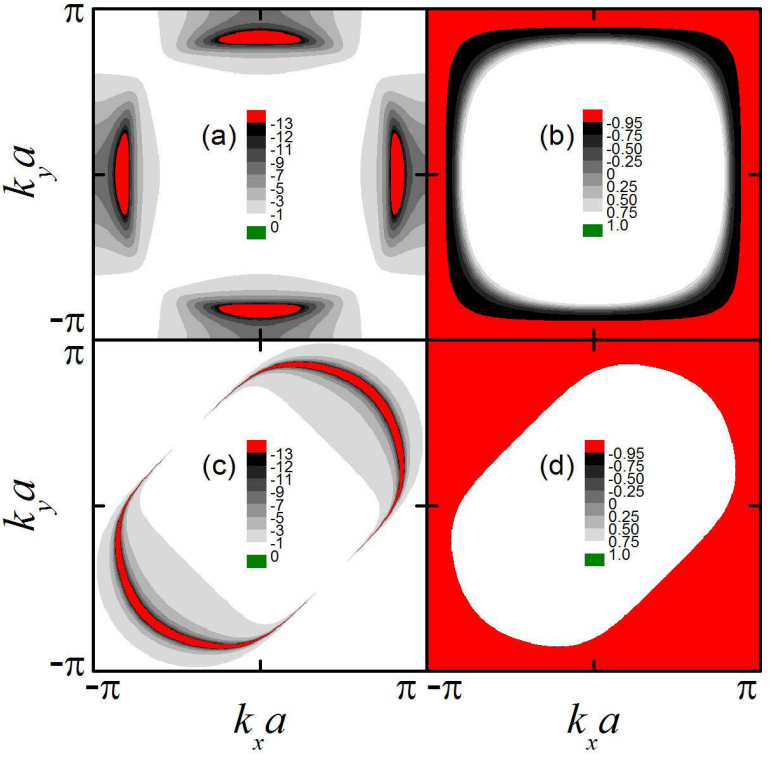

Fig. 1. (Color on line) Contour plots of integrands of (a) Eq. (17) and (b) Eq. (12) for d-wave superconducting states, while (c) Eq. (18) and (d) Eq. (12) for p-wave ones.

Notice that $\Delta t_3^{\pm}$ has no effects on the s-wave superconductivity except for the single-electron dispersion relation. For the d-channel, Eq. (11) can be written as[9]

$$1 = \frac{4\Delta t_3 a^2}{8\pi^2} \int_{-\pi/a}^{\pi/a} \int_{-\pi/a}^{\pi/a} dk_x dk_y \frac{\left[\cos(k_x a) - \cos(k_y a)\right]^2}{E(\mathbf{k})} \tanh\left(\frac{E(\mathbf{k})}{2k_B T}\right) \quad . \quad (17)$$

Likewise, for the p-channel, Eq. (11) leads to[8]

$$1 = \pm\frac{4\delta_3 a^2}{8\pi^2} \int_{-\pi/a}^{\pi/a} \int_{-\pi/a}^{\pi/a} dk_x dk_y \frac{\left[\sin(k_x a) \pm \sin(k_y a)\right]^2}{E(\mathbf{k})} \tanh\left(\frac{E(\mathbf{k})}{2k_B T}\right) \quad , \quad (18)$$

In general, the critical temperature (T_c) is determined by $\Delta_\alpha(T_c) = 0$, being α=s, p or d.

Figures 1(a) and 1(b) respectively show the contour plots of the integrand functions of Eqs. (17) and (12) for $t = -1$, $t' = -0.45|t|$, $\Delta t = 0.5|t|$, $\Delta t_3 = 0.1|t|$, $\delta_3 = 0$, $U = 6|t|$, $n = 1.94$, $k_B T_c = 0.06319|t|$, and $\mu = 6.13585|t|$. Notice that the main contribution to the integral of Eq. (17) comes from the sharp walls located at the Fermi surface defined by $\varepsilon(\mathbf{k}) = \mu$, and separated by d-wave nodes. In contrast,

for Eq. (12) the integrand has a step behaviour around the Fermi surface. Likewise, Figures 1(c) and 1(d) illustrate the contour plots of the integrand functions of Eqs. (18) and (12), respectively, for $t = -1$, $t' = -0.45|t|$, $\Delta t = 0.5|t|$, $\Delta t_3 = 0.1|t|$, $\delta_3 = 0.1|t|$, $U = 6|t|$, $n = 1$, $k_B T_c = 0.00093|t|$, $\mu = 3.307|t|$, and taking the upper sign in Eq. (18). Observe that similar to the previous case, the sharp walls and step behaviour are located at the Fermi surface. However, the Fermi surface is oriented along the $\hat{x} + \hat{y}$ direction, due to the magnitude and sign of δ_3. Furthermore, the step in Fig. 1(d) is sharper than in Fig. 1(b), since the p-channel T_c is smaller than the d-channel one. It would be worth mentioning that the general behaviour shown in figures 1 is not sensitive to the particular Hamiltonian parameter values and they were chosen in order to make comparisons with experimental data, as discussed in the following sections.

4. Results

Fig. 2(a) shows the critical temperature (T_c) as a function of n for s- (open circles), p- (open triangles) and d-symmetry (open squares) superconducting states with $t = -1$, $t' = -0.45|t|$, $\Delta t = 0.5|t|$, and $U = 6|t|$. For s and d symmetries we have taken $\Delta t_3 = 0.1|t|$ and $\delta_3 = 0$; whereas for p symmetry, $\Delta t_3 = 0.15|t|$ and $\delta_3 = 0.1|t|$. Notice that the maximum T_c for the d-channel is located at the optimal $n = 1.73$, similar to that observed in cuprate superconductors since the hole doping concentration x is related to $2 - n$. This relationship is taken for the lower Hubbard sub-band, because the Coulomb repulsion induces a charge-transfer gap in a half filled band.[5] In contrast, for p-channel, the maximum T_c is found around half-filling close to the expected electronic density of $n = 1.2$ for Sr_2RuO_4.[13,14] Furthermore, for s-wave the maximum T_c is found for $n = 1.47$.

The mean potential energy ($\langle Z \rangle$) can be written as[15,16]

$$\langle Z \rangle = \frac{1}{N_s^2} \sum_{\mathbf{k},\mathbf{k}'} Z_{\mathbf{k},\mathbf{k}'} u_{\mathbf{k}} v_{\mathbf{k}}^* u_{\mathbf{k}'}^* v_{\mathbf{k}'} = -\frac{1}{N_s} \sum_{\mathbf{k}} \frac{\Delta_{\mathbf{k}}^2}{2E_{\mathbf{k}}} \quad , \tag{19}$$

where

$$\Delta_{\mathbf{k}} = \frac{1}{N_s} \sum_{\mathbf{k}'} Z_{\mathbf{k},\mathbf{k}'} u_{\mathbf{k}'}^* v_{\mathbf{k}'} \quad , \tag{20}$$

and

$$\frac{\Delta_{\mathbf{k}}}{2E_{\mathbf{k}}} = u_{\mathbf{k}} v_{\mathbf{k}}^* \quad . \tag{21}$$

In Fig. 2(b), we show $\langle Z \rangle$ as a function of n for s- (solid circles), p- (solid triangles) and d-channel (solid squares) with the same parameters of Fig. 2(a). Observe that $\langle Z \rangle$ is negative and its absolute value has almost the same electron-density dependence as T_c, mainly due to the smooth variation of the mean kinetic energy.

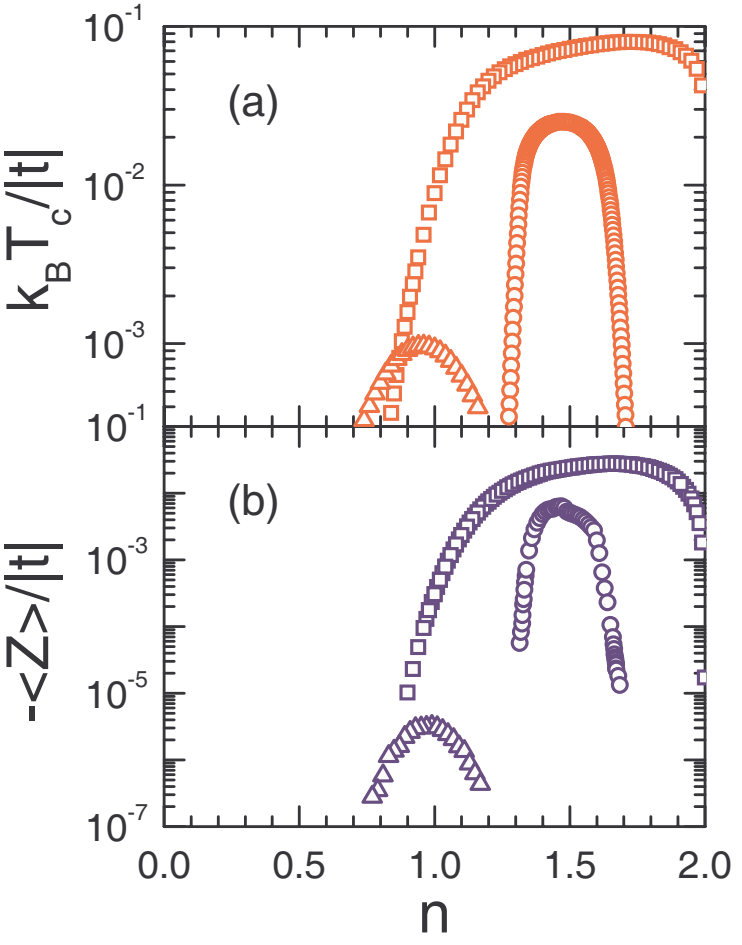

Fig. 2. (a) Critical temperature (T_c) and (b) mean potential energy ($\langle Z \rangle$) as functions of the electron density (n) for s- (solid circles), p- (solid triangles) and d-channel (solid squares).

One of the physical quantities that yields information about the symmetry of superconducting states is the electronic specific heat (C), which is highly sensitive to the low-energy excitations. The C of superconducting states is given by[15]

$$C = \frac{2k_B\beta^2}{4\pi^2} \int\int_{1BZ} f\left(E_{\mathbf{k}}\right)\left[1 - f\left(E_{\mathbf{k}}\right)\right]\left[E_{\mathbf{k}}^2 + \beta E_{\mathbf{k}} \frac{dE_{\mathbf{k}}}{d\beta}\right] dk_x dk_y \quad , \tag{22}$$

where $\beta = 1/(k_B T)$ and $f(E)$ is the Fermi-Dirac distribution. To obtain the specific heat of the normal state we take $\Delta_{\mathbf{k}}$ equal to zero.[15] In Fig. 3, two electronic densities (a) $n = 1.2$ and (b) $n = 1.94$ are chosen from Fig. 2 to calculate their d-channel electronic specific heat and compared with experimental data obtained from $La_{2-x}Sr_xCuO_4$ for $x = 0.22$ and $x = 0.1$, respectively.[17] Insets of Fig. 3 show

the corresponding theoretical angular dependences of the single-excitation energy gap (Δ) defined as the minimum value of $E_{\mathbf{k}}$ in $\mathbf{k}$ direction.[8] The polar angle is given by $\theta = \tan^{-1}(k_y/k_x)$. Notice that for the hole overdoped regime, $n < 1.73$, Δ has a $d_{x^2-y^2}$ symmetry and in consequence C is proportional to T^2 as obtained in Ref. 18. However, for the hole underdoped regime ($n > 1.73$) Δ has a d_{xy}-like symmetry without real nodes and then, C has an exponential behaviour as occurs in an s-wave superconductor. The residual C/T value at $T = 0$ in experimental data could be due to the chemical or electronic inhomogeneity of the sample,[17,19] and this fact is not considered in the theory.

Finally, Fig. 4 shows the electronic specific heat (C) for the same p-wave system of Fig. 2 with $n = 1.0$ in comparison with the experimental data obtained from the spin-triplet superconductor Sr_2RuO_4.[20] Inset of Fig. 4 illustrates the angular dependence of the single-excitation energy gap. Notice the remarkable agreement in both, the discontinuity at T_c and the temperature dependence below T_c, as a consequence of the nature of the p-wave superconducting state. In fact, a power-law temperature dependence $C(T) \sim T^{\alpha}$ with $\alpha < 2$ is observed, which could be related to the wider depleted-gap region compared with the d-wave case.

5. Conclusion

We have presented a unified theory of the s-, p- and d-wave superconductivity based on the BCS formalism and a generalized Hubbard model. This approach has the advantage of being simple and general for predicting the trends of anisotropic superconducting materials properties. Moreover, it does not require attractive density-density interactions and the superconductivity is originated by the correlated hoppings interactions. In spite of their small strength in comparison with other terms of the Hamiltonian, they determine the symmetry of the superconducting ground states. The superconducting properties are calculated by solving two coupled integral equations when the variation of the chemical potential is considered. The main contribution to the involved integrals comes from a sharp wall located around the Fermi surface, in consistence with the BCS theory.[1,15] There is a maximum T_c located at low, medium and high electron densities for p, s and d symmetry superconductivity, respectively; in qualitative agreement with the experimental data.[2,4] In particular, positive Hall coefficients are observed[21,22] in d-wave high-T_c superconductors indicating its superconductivity could be originated from hole carriers. On the other hand, the low-temperature behavior of C is very sensitive to the existence of nodes in the superconducting gap as well as their deepness. In particular, the results show that the d-channel C in the overdoped regime has a second-order power-law behavior, whereas in the underdoped regime C has an almost exponential temperature dependence, similar to the s-channel case, due to the absence of real nodes in the superconducting gap. In fact, the d_{xy}-like gaps without real nodes have been observed in cuprate superconductors by scanning tunneling experiments.[23] In addition, p-channel C shows a sub-second-order power-law behaviour

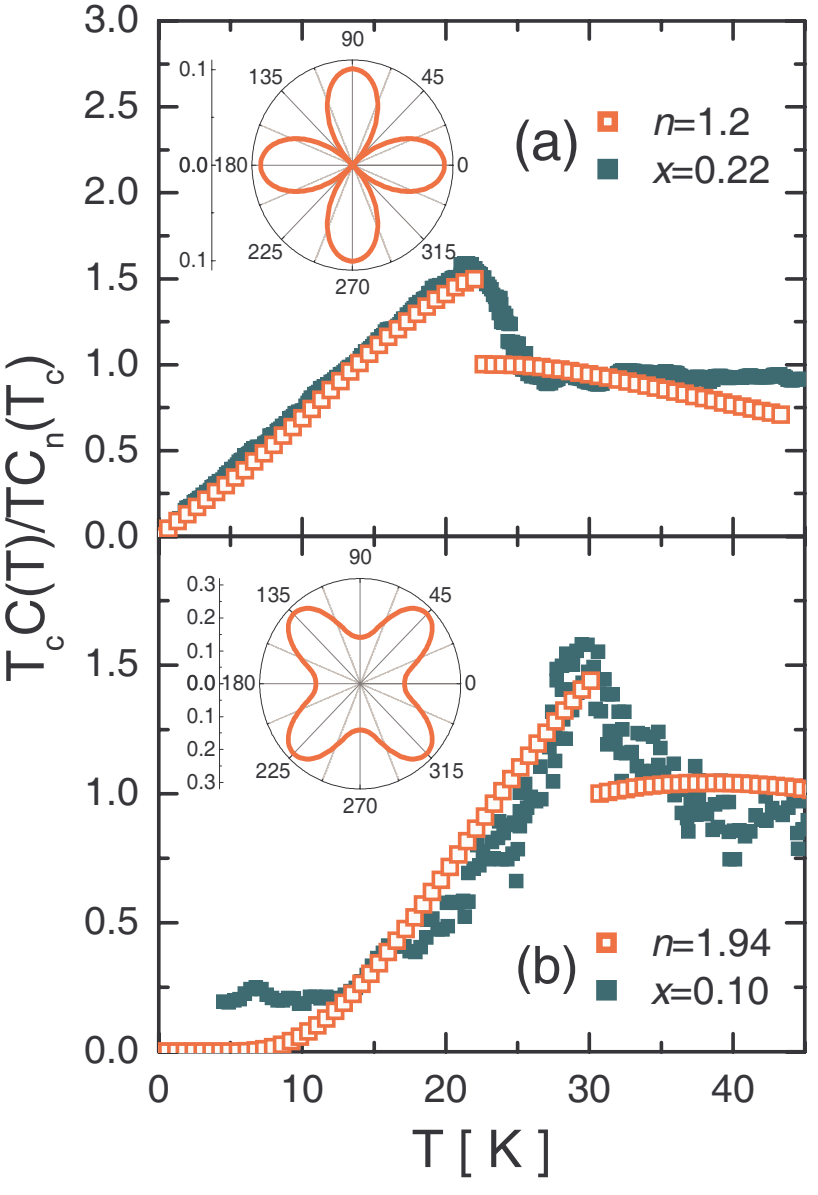

Fig. 3. Theoretical (open squares) d-wave electronic specific heat (C) versus temperature (T) for the same d-wave systems as in Fig. 2 with (a) $n = 1.2$ and (b) $n = 1.94$, in comparison with experimental data (solid squares) obtained from $La_{2-x}Sr_xCuO_4$ for (a) $x = 0.22$ and (b) $x = 0.1$.[17] Insets: Corresponding single-excitation energy gaps ($\Delta/|t|$) as a function of the polar angle (θ).

as obtained in Sr_2RuO_4. We expect that this analysis could contribute the understanding of the different $C(T)$ behaviors observed in anisotropic superconductors.

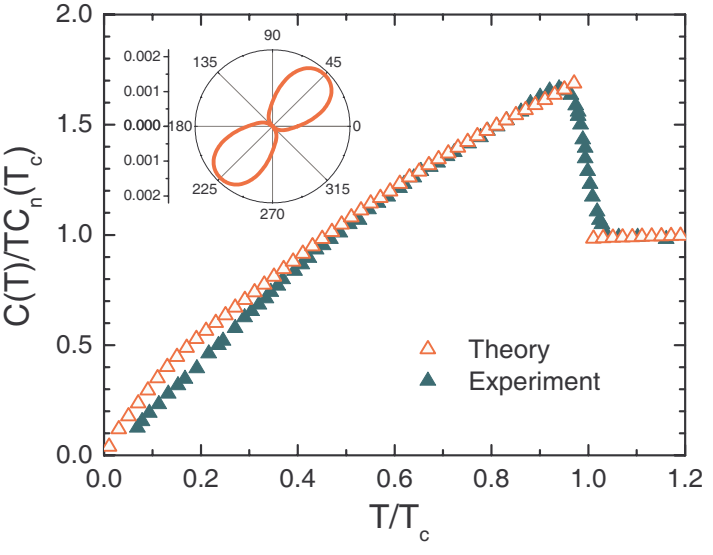

Fig. 4. Theoretical (open triangles) p-wave specific heat (C) calculated by using the same parameters of Fig. 2 with $n = 1.0$, versus temperature (T) in comparison with the experimental data (solid triangles) obtained from Sr_2RuO_4.[20] Inset: Single-excitation energy gap ($\Delta/|t|$) as a function of the polar angle (θ).

The present study can be extended to include the effects of external perturbations, such as magnetic fields, on the physical properties of anisotropic superconductors. This extension is currently being developed.

Acknowledgments

This work has been partially supported by CONACyT-58938, UNAM-IN113008, UNAM-IN114008 and the UNAM-UNACAR exchange project. Computations have been performed at Bakliz and KanBalam of DGSCA, UNAM.

References

1. J. Bardeen, L. N. Cooper and J. R. Schrieffer, *Phys. Rev.* **108**, 1175 (1957).
2. C. C. Tsuei and J. R. Kirtley, *Rev. Mod. Phys.* **72**, 969 (2000).
3. K. D. Nelson, Z. Q. Mao, Y. Maeno and Y. Liu, *Science* **306**, 1151 (2004).
4. A. P. Mackenzie and Y. Maeno, *Rev. Mod. Phys.* **75**, 657 (2003).
5. H. -B. Schüttler and A.J. Fedro, *Phys. Rev. B* **45**, 7588 (1992).
6. J. F. Annett, G. Litak, B. L. Gyorffy and K. I. Wysokinski, *Phys. Rev. B* **66**, 134514 (2002).
7. I. I. Mazin and D. J. Singh, *Phys. Rev. Lett.* **79**, 733 (1997).
8. J. S. Millán, L. A. Pérez and C. Wang, *Phys. Lett. A* **335**, 505 (2005).
9. L. A. Pérez and C. Wang, *Solid State Commun.* **121**, 669 (2002).
10. R. Matzdorf, Z. Fang, Ismail, J. Zhang, T. Kimura, Y. Tokura, K. Terakura, and E. W. Plummer, *Science* **289**, 746 (2000).

11. E. Dagotto, J. Riera, Y. C. Chen, A. Moreo, A. Nazarenko, F. Alcaraz, and F. Ortolani, *Phys. Rev. B* **49**, 3548 (1994).
12. J. E. Hirsch and F. Marsiglio, *Phys. Rev. B* **39**, 11515 (1989).
13. T. Oguchi, *Phys. Rev. B* **51**, 1385 (1995).
14. D. J. Singh, *Phys. Rev. B* **52**, 1358 (1995).
15. M. Tinkham, *Introduction to Superconductivity* (2nd Edition, McGraw Hill, New York, 1996).
16. G. Rickayzen, *Theory of Superconductivity* (Wiley, New York, 1965).
17. T. Matsuzaki, N. Momono, M. Oda, and M. Ido, *J. Phys. Soc. Jpn.* **73**, 2232 (2004).
18. H. Won and K. Maki, *Phys. Rev. B* **49**, 1397 (1994).
19. H.-H. Wen, Z.-Y. Liu, F. Zhou, J. Xiong, W. Ti, T. Xiang, S. Komiya, X. Sun, and Y. Ando, *Phys. Rev. B* **70**, 214505 (2004).
20. S. Nishizaki, Y. Maeno, and Z. Mao, *J. Phys. Soc. Jpn.* **69**, 572 (2000).
21. H. Y. Hwang, B. Batlogg, H. Takagi, H. L. Kao, J. Kwo, R. J. Cava, J. J. Krajewski, and W. F. Peck, Jr., *Phys. Rev. Lett.* **72**, 2636 (1994).
22. F. F. Balakirev, J. B. Betts, A. Migliori, S. Ono, Y. Ando, and G. S. Boebinger, *Nature* **424**, 912 (2003).
23. J. Kane and K. W. Ng, *Phys. Rev. B* **53**, 2819 (1996).